Volume 1 | Number 1 | Jan 2013 | Pages 1–100

Nanoscale

www.rsc.org/nanoscale

ROYAL SOCIETY OF CHEMISTRY

ROYAL SOCIETY OF CHEMISTRY

www.rsc.org/nanoscale

Nanoscale

ARTICLE

ANTIFUNGAL NANOFIBERS MADE BY CONTROLLED RELEASE OF SEA ANIMAL DERIVED PEPTIDE

Juliane F. C. Viana[a,b], Jéssica Carrijo [b], Camila G. Freitas[b,c], Arghya Paul[d], Jarib Alcaraz[e], Cristiano C. Lacorte[f], Ludovico Migliolo[b], César A. Andrade[e], Rosana Falcão[f], Nuno C Santos[g], Sónia Gonçalves[g], Anselmo J. Otero-González[h], Ali Khademhosseini[d], Simoni C. Dias[b] and Octávio L. Franco[a,b, i]*

Candida albicans is a common human-pathogenic fungal species with ability to cause several diseases including surface infections. Despite the clear difficulties of *Candida* control, antimicrobial peptides (AMPs) have emerged as an alternative strategy for fungal control. In this report, different concentrations of antifungal Cm-p1 (*Cencritchis muricatus* peptide 1) were electrospun in nanofibers for drug delivery. Nanofibers were characterized by mass spectrometry confirming peptide presence on the scaffold. Atomic force microscopy and scanning electronic microscopy were used for diameter measures showing that Cm-p1 affects fiber morphology as well as diameter and scaffold thickness. The Cm-p1 release behavior from nanofibers demonstrated peptide release from 30 min until three days, leading to effective yeast control in the first 24 hours. Moreover, biocompatible fiber was evaluated though MTS assay as well ROS production by using a HUVEC cell model, showing that fiber does not affect cell viability and only nanofibers containing 10 % Cm-p1-PVA improved ROS generation. In addition, the secretion of pro-inflammatory cytokines IL-6 and TNF-α by HUVECs was also slightly modified by 10 % Cm-p1-PVA nanofiber. In conclusion, the electrospinning technique here applied allowed for the manufacture of biodegradable biomimetic nanofibrous extracellular membranes with the ability to control yeast infection.

Notes and references

[a] Programa de Pós-Graduação em Patologia Molecular, Universidade de Brasília, Brazil
[b] Programa de Pós-Graduação em Ciências Genômicas e Biotecnologia, Centro de Análises Proteômicas e Bioquímicas, Universidade Católica de Brasília, Brazil.
[c] Instituto Federal de Educação, Ciência e Tecnologia de Brasília, Brasília, Brazil.
[d] Biomaterials Innovation Research Center, Division of Biomedical Engineering, Brigham and Women's Hospital, Harvard Medical School/Wyss Institute for Biologically Inspired Engineering/Harvard-MIT Division of Health Sciences and Technology, Massachusetts Institute of Technology, Cambridge, USA
[e] Programa de Pós-Graduação em Ciências dos Materiais, Universidade Federal de Pernambuco, Recife, Brazil.
[f] EMBRAPA Recursos Genéticos e Biotecnologia, Parque Estação Biológica, Brasília, Brazil.
[g] Instituto de Medicina Molecular, Faculdade de Medicina, Universidade de Lisboa, Lisbon, Portugal
[h] Centro de Estudios de Proteínas, Facultad de Biología, Universidad de La Habana, Cuba.
[i] Pos-Graduacao em Biotecnologia, Universidade Catolica Dom Bosco, Campo Grande, MS, Brazil

*Corresponding author: Octávio Luiz Franco, Centro de Análises Proteômicas e Bioquímicas, Pós-Graduação em Ciências Genômicas e Biotecnologia. SGAN 916 Av. W5 Norte - Modulo C - Sala 222, CP 70790-160 - Brasília, DF – Brazil. E-mail: ocfranco@gmail.com

INTRODUCTION

Candida spp. are known to cause opportunistic infections in immunocompromised patients [1, 2]. *Candida albicans* is considered the most common human-pathogenic fungal species, causing several diseases including life-threatening bloodstream and painful superficial infections[3, 4]. Moreover, invasive candidiasis has been considered a significant cause of late-onset infection in premature infants[5]. Candidiasis is also known as the major cause of mortality and morbidity in immunocompromised patients as a result of AIDS, cancer chemotherapies or organ transplantation[4, 6]. Despite the advances in treatment and management of fungal infections, there are several reports about resistant fungal strains, treatment failure

and the scarcity of antifungal agents with low toxicity for systemic *C. albicans* infections[6].

Despite the clear difficulties of *Candida* control, antimicrobial peptides (AMPs) have emerged as alternative compounds for pathogen control. These proteinaceous compounds show a wide spectrum of activities against pathogenic bacteria, fungi, viruses, parasites, besides analgesic and immunomodulatory activities[7-9]. Cm-p1 (SRSELIVHQR) is an AMP isolated from *Cenchritis muricatus*, a snail-like Caribbean sea mollusk [10] with bactericidal activity against *Staphylococcus aureus* and *Escherichia coli*. In complementary studies, Cm-p1 was chemically synthesized, functionally characterized and further evaluated regarding its antimicrobial activities, showing deleterious activities against yeasts and filamentous fungi. Moreover, no toxicity against human red blood and RAW 264.7 cells was noted[11].

For AMPs to function properly, they must be delivered with appropriate dosage and time, which remains a significant challenge. Several works report the self-assembling peptides in nanofibers for tissue engineering[12], drug release[13] and biomaterial[14] production. Moreover, the use of electrospun nanofibers has been investigated as a potential wound dressing, since the fibrous structure can protect wounds from microbial contamination, making it possible to incorporate antimicrobial agents, growth factors and antiseptics [15, 16]. Antibiotics incorporated in electrospun nanofibers include silver compounds[17-20], vancomycin [21, 22], gentamicin [21-23] and rifampicin[24]. However, some AMPs have also been employed in electrospun nanofiber mats[13, 25-30]. Electrospinning is a promising tool for peptide nanofiber production[31]. This process allows nanofiber fabrication of diverse materials with diameters ranging from nanometers to micrometers, with high porosity, large surface area[17, 32] and efficient controlled drug release[31]. Here, the electrospinning feasibility for a synthetic antimicrobial peptide Cm-p1 in nanofibers of poly(vinyl alcohol) was explored in order to generate an antifungal wound dressing with protective activity against *Candida*. Furthermore, immunomodulatory activities, cellular viability and reactive oxygen species generation with different scaffold formulations were also determined. The scaffolds were further characterized by scanning electron and atomic force microscopies as well as by MALDI-ToF technology.

RESULTS AND DISCUSSION

Electrospun fiber mats of PVA/Cm-p1 and peptide detection

Cm-p1-PVA-loaded nanofibrous membrane was fabricated by electrospinning PVA. During the electrospinning process, parameters such as voltage and distance between the needle and the collector were kept the same for every PVA and Cm-p1-PVA fiber. Earlier, Cm-p1 was solubilized in deionized water under stirring (200 rpm) and then 10 % PVA was added to the peptide solution. The hydrophilic nature of Cm-p1 allowed its solubilization in deionized water. PVA, a synthetic polymer, has been widely used to produce electrospun fiber mats [33] attracting attention due to biocompatibility, hydrophilicity, physical properties and chemical resistance [34, 35]. Furthermore, PVA nanofibers have been applied in different fields, such as enzyme immobilization, electrode materials, sensors and biomedical applications[36, 37].

Firstly, MALDI ToF analyses of fibers were performed in order to identify the existence or absence of Cm-P1. Figure 1a demonstrates the free Cm-p1 molecular mass (1,224.48 Da). Moreover, identical molecular mass was obtained by directly ionizing the nanofiber containing Cm-p1-PVA (Figure 1b). The resulting observations reinforce the idea that the peptide is encapsulated within the fiber through weak interactions. The PVA fiber free of peptide was also checked, demonstrating the complete absence of Cm-p1 (Figure 1c).
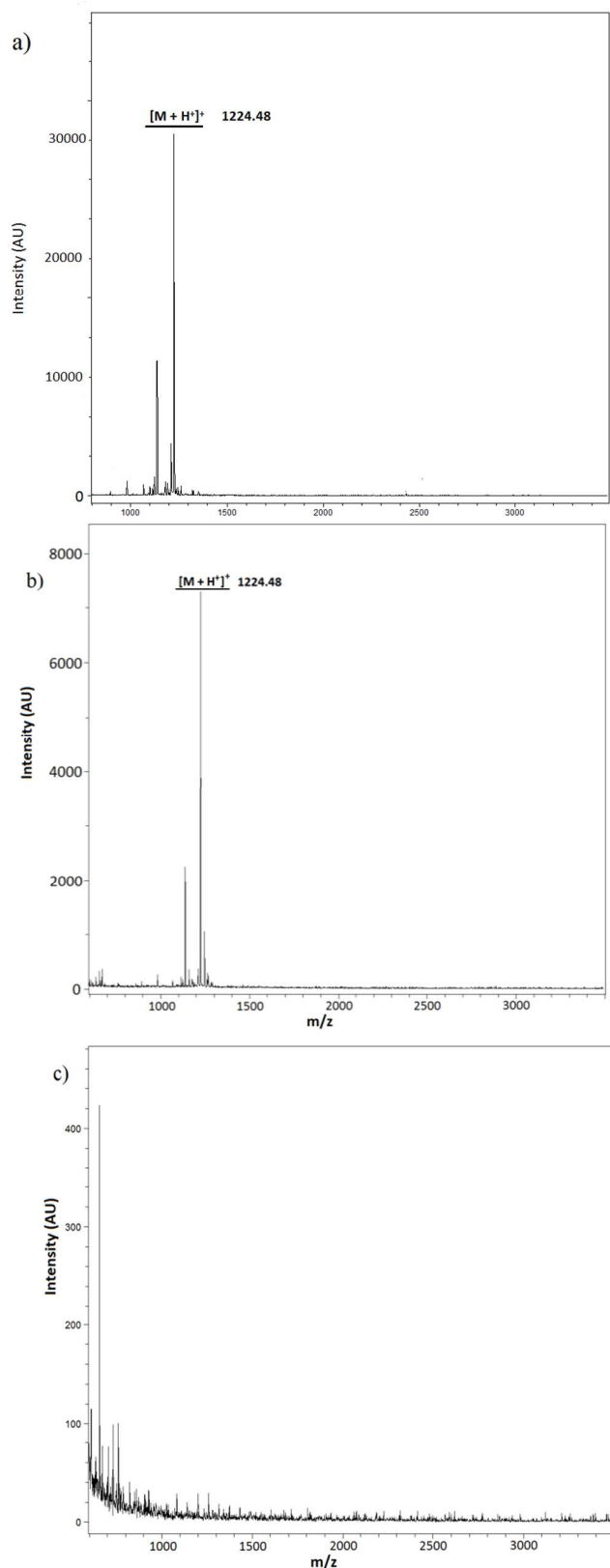
Fig. 1 MALDI ToF analysis of (**a**) free Cm-p1, (**b**) Cm-p1-PVA incorporated in elestrospun nanofiber and (**c**) PVA nanofiber with no peptide.

Microscopic characterization of fibers

To better evaluate the resulting fibers, SEM was performed (Figure 2a, 2b). SEM micrographs in other magnifications can be seen in Supplementary Figure 1. The average diameters of spun fibers containing Cm-p1-PVA were 295.3 ± 44.9 nm, 293.5 ± 45.8 nm, 210.6 ± 47.1 nm for the concentrations of 2.5 % Cm-p1-PVA, 5 % Cm-p1-PVA and 10 % Cm-p1-PVA, respectively. Otherwise, for PVA fibers without Cm-p1, the diameter average was 335.9 ± 28.2 nm. The nanofiber image characterizations in Fig. 2a and Fig. 2b show that fiber diameters decrease with the presence of Cm-p1 when compared with PVA fiber mat. Furthermore, the standard deviation observed in control fibers was less than that in fibers containing the peptide, indicating that PVA control fibers are more homogeneous and bead-free in comparison to fibers containing Cm-p1.
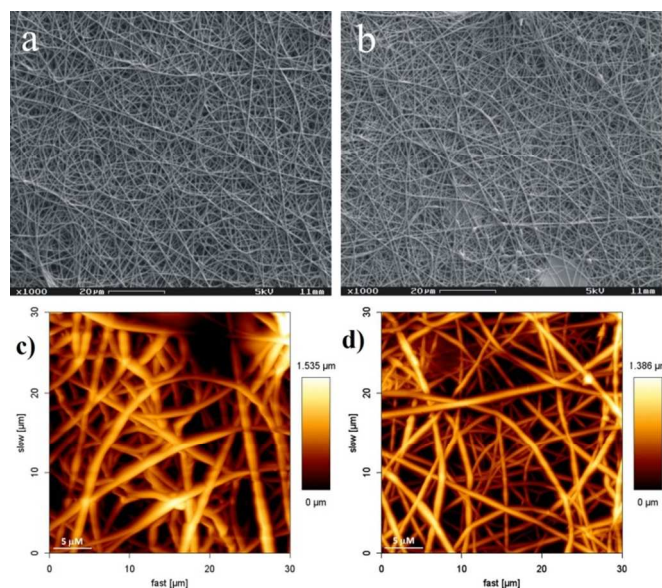
Fig. 2 SEM and AFM micrographs of PVA and Cm-p1-PVA fibers. (a) 10 % PVA fibers in 1000x magnification by SEM, (b) 10 % Cm-p1- PVA fibers in 1000x magnification by SEM, (c) 10 % PVA fibers by AFM and (d) 10 % Cm-p1- PVA fibers by AFM.

AFM was also used for further sample characterization since this technique can be used to measure soft and fragile adhesive surfaces, without harming samples[38]. Indeed, AFM images (Fig 2c, 2d) confirmed SEM results, showing that the thickness of nanofibers containing 10 % Cm-p1-PVA (Fig 2b) is smaller than PVA (Fig 2a)

Nanoscale Accepted Manuscript

spun fibers, presenting 1386 nm and 1535 nm, respectively. In complementary measurements, the fiber diameters were also evaluated by AFM (Fig 2c, 2d). As in SEM measures, 2.5 % Cm-p1-PVA (570.8 ± 81.6 nm) and 10 % Cm-p1-PVA (550.2 ± 144.4 nm) samples presented smaller diameters than control samples (990.9 ± 128.9 nm). However, by AFM, the diameter measurements were higher than SEM in every sample analyzed. It is possible that during SEM measurements samples are dehydrated, decreasing fiber diameters. Significance between PVA and Cm-p1-PVA fibers measures were found (**$P < 0.0001$) in SEM and AFM measures. Furthermore, the nanofibers were not uniform in the case of the 10 % Cm-p1-PVA sample, according to Fig 2a and Fig 2b, suggesting that high concentrations of Cm-p1 may interfere in fiber morphology due to the insufficient stretching of the polymer jet during the electrospinning process through jet suspension and needle obstruction, leading to bead formation in 10 % Cm-p1-PVA mats. Nanofibers containing the antimicrobial peptide nisin also displayed a smaller diameter when compared with control fibers[27].

Peptide nanofiber release

The peptide release from Cm-p1-PVA nanofiber mats with different Cm-p1 contents is shown in Fig 3. The Cm-p1 release behavior from nanofibers demonstrated peptide release from 30 min until three days, leading to effective yeast control in the first 24 h. Cm-p1 was rapidly released from Cm-p1-PVA-loaded electrospun nanofiber mats. Fig 3a shows that after 120 min, Cm-p1 was released into the dissolution medium from 2.5, 5 and 10 % Cm-p1-PVA nanofiber mats (Fig 3a). In parallel, for cumulative peptide release, another nanofiber fragment was incubated in a glass tube at 37 °C, the buffer was changed every 24 h until 3 days without removal, and the Cm-p1 amount was quantified. Fig 3b shows that the release of Cm-p1-PVA spun fibers was higher during the first 24 h, gradually decreasing after 48 and 72 h, probably due to a reduction in peptide concentration inside the fiber mat. Supplementary Figure 2 presents Cm-p1 quantification by using HPLC chromatograms after 24 h of release; the quantified nanofiber release at every time evaluated with the triplicate media and standard deviation is shown in Supplementary Table 1. Every sample was quantified by HPLC and the chromatograms do not show any alteration and modification in the spectrum, suggesting that during the release assay the peptide was stable. These values were also used to calculate the peptide quantity for antifungal assays. It is of interest

that Cm-P1 release was sustained after 48 h, which could be a desirable property for anti-infective biomaterials. PVA nanofibers could provide a fast-dissolving hydrophilic environment. The fast release of Cm-p1-PVA from the nanofiber can be triggered by extremely high surface area and porosity of the scaffolds. However, some studies suggest crosslinking PVA, aiming to decrease the PVA hydrophilicity and then increasing the dissolution time of PVA fibers [34, 39, 40]. The synthetic AMP fluorescein labelled inverse-Crabrolin (iCR-fluor) was incorporated into electrospun poly(ε-caprolactone) and presented 30 % release rate in the first 30 min. After 2 h, the release of the encapsulated molecule was 50 % [25]. The accumulative release of plantaricin 423 from electrospun blends poly(D,L-lactide) and poly(ethylene oxide) was evaluated by Heunis and colleagues [26] and exhibited a high initial burst release and a more continuous release of bacteriocin over an 8-day period.
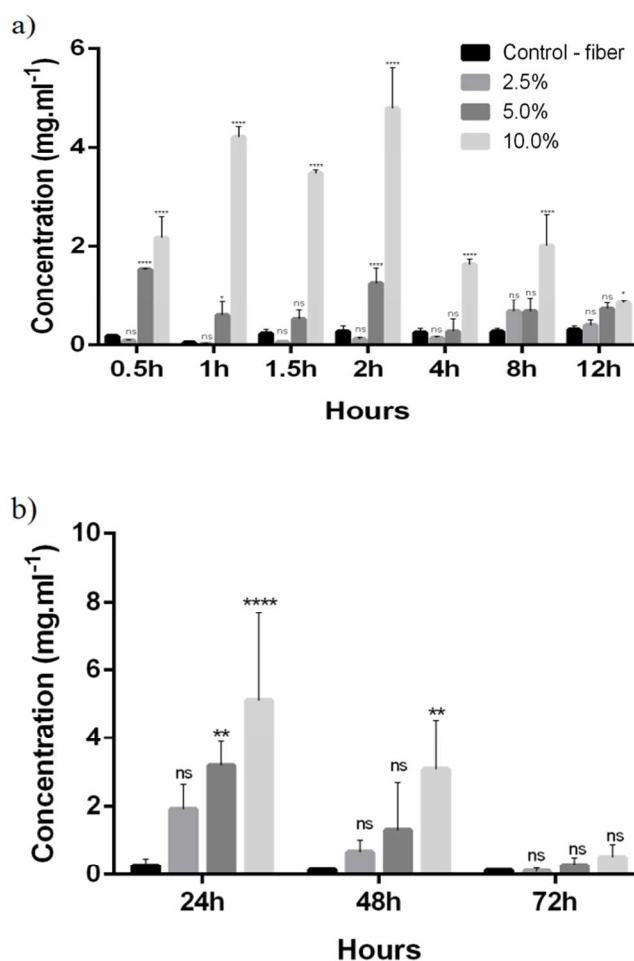
Fig. 3 Cm-p1-PVA release analyses from nanofibrous membranes (a) using different scaffolds in hours and (b) from the same scaffolds until 72 hours. NS: no significance. (*$P < 0.1$; **$P < 0.01$; ****$P < 0.0001$).

Antifungal activity

The activity of antifungal Cm-p1-PVA loaded nanofibers against *C. albicans* was evaluated by radial diffusion assay (RDA) by comparing the inhibition halo between amphotericin 30 mg.ml^{-1}, free Cm-p1 and the PVA and Cm-p-PVA fiber mats. The Cm-p1 concentrations were evaluated by HPLC from release quantification in 24 h and then used for bioassay. A quantitative list of antifungal activities of the different loading agents and the ratio inhibition measures is presented in Table 1. In a previous assay, no halo was visualized when fibers were added directly to Sabouraud dextrose plate (data not shown). Only 10 % Cm-p1-PVA nanofibers were able to inhibit *C. albicans* growth after the nanofibers had been solubilized in distilled water. Despite Cm-p1 activity, previous results[11] presented higher activity than 10 % Cm-p1-PVA nanofibers. According to Hassounah and co-workers [41], the establishment of hydrogen bonds between the amino groups of the drugs and the alcohol groups of PVA can lead to deactivation of drugs due to the high polarity of the alcoholic oxygen atom in PVA. [41] In a preceding theoretical structural analysis[11] it was predicted that Cm-p1 consists of a hydrophilic molecule scoring an impressive average of hydropathicity and displays a minor central hydrophobic region bordered by basic amino acids at the extremes[11]. A three-dimensional theoretical model of Cm-p1 revealed an α-helix conformation with a distribution of net charge caused by exposed cationic histidine (His8) and arginine (Arg2 and Arg10) residues. Leucine (Leu5) and valine (Val7), the hydrophobic preserved region, seem to perform a critical role in the peptide's antifungal activity, favoring peptide-membrane interaction[11]. Furthermore, the amino acid residue Val7 can be significant in fungal interaction. Studies demonstrated that the pleurocidin lethal effects against *Candida albicans* and other fungi occurs due to the presence of amidated valine residue at the C-terminus [42]. This same effect was also visualized with antimicrobial peptide adenoregulin against filamentous fungi and Gram-positive and negative bacteria [43].

Table 1 Quantitative list of nanofiber scaffolds with respective to concentration and halo inhibition in Sabouraud dextrose agar measures against *C. albicans* ATCC 10231.

Compound	Concentration (mg.mL^{-1})	Ratio inhibition measure [44]
Amphotericin	30.00 mg.mL^{-1}	14.10 mm
Free Cm-p1	4.00 mg.mL^{-1}	9.27 mm
PVA fiber	N/A	N/D
2.5 % Cm-p1- PVA fiber	1.92 mg.mL^{-1}	N/D
5 % Cm-p1- PVA fiber	3.04 mg.mL^{-1}	N/D
10 % Cm-p1- PVA fiber	5.26 mg.mL^{-1}	3.94 mm

Note: N/A: not applicable; N/D: not detectable

Biocompatibility of Cm-p1- PVA fiber with mammalian cells

HUVEC viability (Fig 4a) was evaluated in the presence of different nanoscaffolds (same peptide/polymer ratio used in the bioassay) using MTS Assay. None of the concentrations of Cm-p1 scaffolds that were tested affected HUVEC viability when compared with PVA scaffolds. These results confirm preliminary studies conducted by López-Abarrategui and colleagues[11], where similar results were observed using free Cm-P1 against RAW 264.7 murine macrophage-like cells. However, the proliferation of HUVECs was affected in the presence of 10% Cm-p1- PVA scaffolds, as shown in Fig 4c. Meanwhile, for PVA fiber, 2.5 % Cm-p1-PVA and 5% Cm-p1-PVA peptide concentrations did not induce significantly lower cell attachment and proliferation in primary endothelial cells.

b)
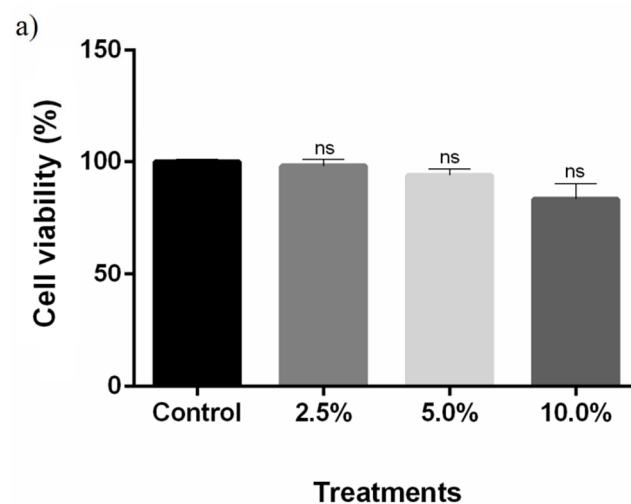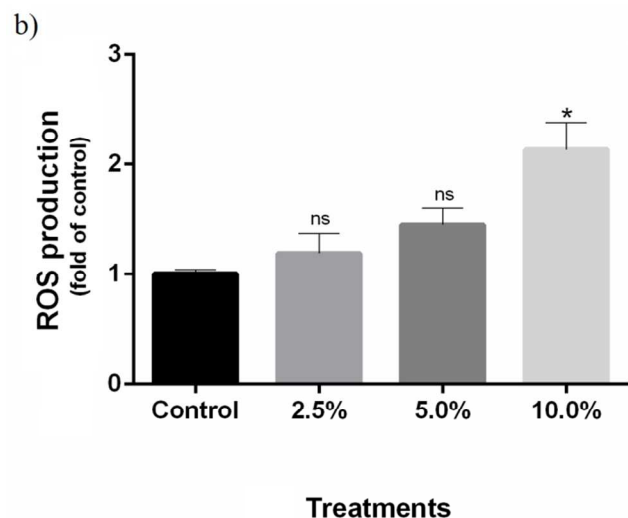
C)
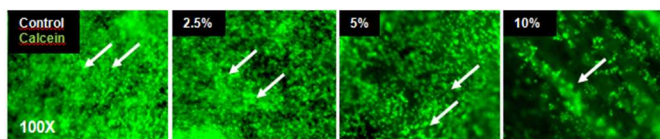
Fig. 4 Biocompatibility of peptide/nanoscaffolds with mammalian cells. Evaluation of (a) HUVEC viability; toxicity profiles of control scaffold (no peptide) and peptides with different concentrations in HUVECs. Relative viability was determined by using the MTS assay and all values were normalized to the values obtained with control group. (b) ROS generation with different scaffold formulations was determined by ROS assay and represented as fold change compared to control. (c) Viable HUVECs (in green) in different nanoscaffold groups stained with calcein AM dye, with less cell attachment and proliferation noted in 10% group (white arrows) compared to others. Data represent mean ± SD. NS: no significance. (*$P < 0.1$).

Moreover we also tried to better explore the mechanism of action of the peptide fiber here analyzed. Since some antimicrobial peptides act by inducing cell death through reactive oxygen species (ROS) production, we evaluated the ROS production by HUVEC cells after 24 h (Figure 4b). This analysis was performed using the same proportion used for the activity assay (2.5%, 5% and 10%). Only 10 % Cm-p1-PVA scaffolds induced the formation of toxic ROS by HUVECs (Fig 4b). Similar data had previously been obtained by using PvD, an antifungal defensin peptide with activity against *C. albicans* from *Phaseolus vulgaris* seed. This peptide induces fungal cell death by membrane permeabilization and the stimulation of oxidative stress injury, with the generation of ROS and nitric oxide [45, 46]. This same mechanism was also described for another plant defensin, HsAFP1 from *Heuchera sanguinea* [44], which

induces several pro-apoptotic signals including ROS accumulation, leading to cell death. Unlike Cm-p1, both HsAFP1 and PvD were able to induce fungal cell death by ROS generation in low concentrations, using 5 μg.mL^{-1} and 100 μg.mL^{-1}, respectively. According to the data in Fig 4b and bioassay results, it is possible that the Cm-p1 mechanism of action may involve ROS generation due to an improvement in production (Figure 4b). However, further studies are needed to confirm this proposition.

Furthermore, nanofiber hemolytic activity was evaluated after 24 h of release (Supp. Fig. 3). No concentrations (2.5%, 5% and 10%) of nanofibers induced hemoglobin leakage. In the same way, in brief experiments[11], no concentrations of free Cm-p1 were capable of causing hemolysis[11]. Antifungal medicines have several toxicity problems against mammalian cells. The authors[11] affirm that this outcome is probably due to the low hydrophobicity of Cm-p1[11].

The secretion of pro-inflammatory cytokines, TNF-α (Fig 5a) and IL-6 (Fig 5b), from RAW 264.7 macrophages after 24h of exposure with control scaffolds (no peptide) and scaffolds carrying different concentrations of Cm-p1 was evaluated. Only 10 % Cm-p1-PVA scaffold presented significant cytokine generation when compared with no peptide scaffolds. However, this production is 3 and 4 times lower for IL-6 and TNF-α respectively, in comparison to the LPS-stimulated group. Moreover, the production of proinflammatory cytokines, such as IL-6 and TNF-α, plays an important role, leading to inflammatory response by inducing other antiinflammatory mediators, the activation of Tcells and the secretion of antibodies by B cells[47].

In this context, the capacity to induce secretion of cytokines to promote the recruitment of immune cells of cathelicidins is well known. The release of TNF-α and IL-6 was induced by cathelicidin LL-37 in keratinocytes and immature dendritic cells at much lower concentrations[48, 49]. Furthermore, the bacteriocin plataricin A, produced by *Lactobacillus plantarum*, was also shown to increase migration and cell proliferation, as well as stimulating the expression of vascular endothelial growth factor A and IL-8 in keratinocytes [50]. Kindrachuk *et al.*[51] demonstrated that nisin Z presents immunomodulatory activities and modulates the host immune response similarly to natural host defense peptides. Although Cm-p1 slightly induces IL-6 and TNF-α secretion in mammalian cells in higher concentrations, this peptide did not present detectable cytotoxicity. In addition, TNF-α and IL-6

production was seen after 24h of cell culture incubation, where the peptide release, shown in Fig. 3b, is 5.26 mg.mL^{-1}. However, after this period the peptide release decreased greatly, reaching insignificant in 72h of cell culture incubation (Fig. 3b). The cytokine production can be minimized, exposing the cells to nanofibers after 24 h, when the Cm-p1 concentration drops. Nevertheless, it is important to emphasize that Cm-p1 activity will also be minimized. In this way, the induction of low pro-inflammatory cytokine production happens only in the early period of its use, helping in the microorganism's elimination and/or prevention. The low cytokine production favors the opsonization of pathogens, the clearance of apoptotic cells and the activation of complement[47, 52].

a)

b)
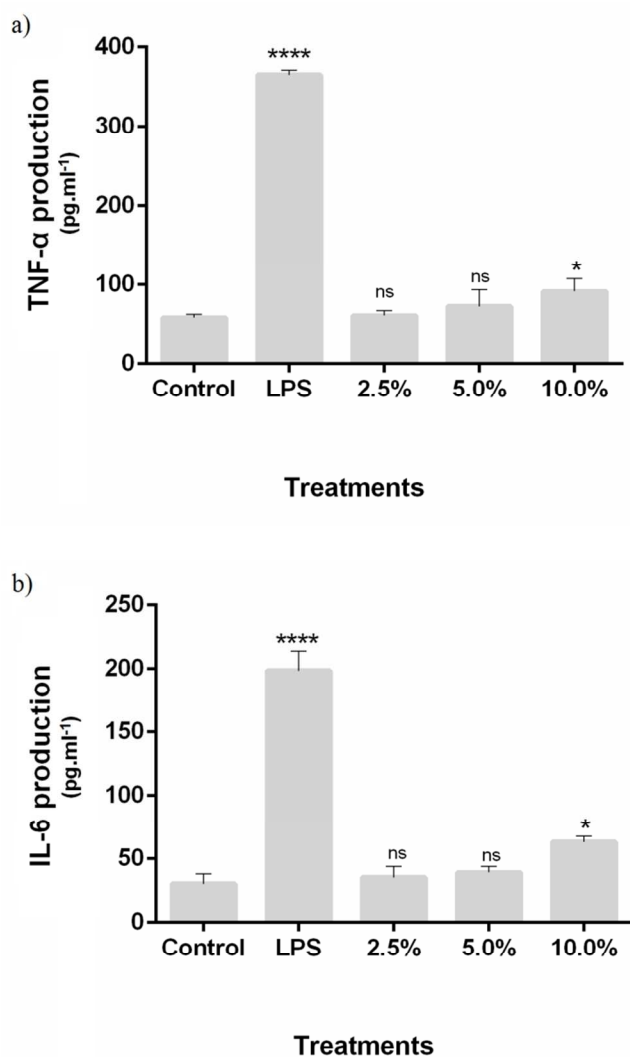
Fig. 5 Evaluation of cytokine pro-inflammatory secretion TNF-α (a) and IL-6 (b) by RAW 264.7 macrophages, after 24h of exposure with control scaffolds (no peptide) and scaffolds carrying different percentages of peptides as obtained by ELISA analysis. LPS was used as positive control. Data represent mean ± SD. NS: no significance. (*$P < 0.1$; ****$P < 0.0001$).

CONCLUSIONS

In this report we describe the production of nanofibers that encapsulate antifungal peptides. At the moment, few antimicrobial peptides have been incorporated in nanofibers[53] and the use of the electrospinning tool should be explored through the incorporation of antimicrobial peptides. In summary, 10 % Cm-p1-PVA concentration was able to decrease *C. albicans* growth. Moreover, in this same concentration, Cm-p1 slightly induced ROS generation without affecting cell viability, as well as being capable of causing low induction of IL-6 and TNF-α production by mammalian cells. Electrospun fibers generated here may be useful as wound care and drug delivery systems. The emerging field of intelligent nanomaterials for medical applications has gained attention in recent decades. However, preclinical development is still a bottleneck to be solved for these advances to reach clinical application.

EXPERIMENTAL

Materials

Polyvinyl alcohol (PVA) with hydrolysis degree of 89 % and molecular mass of 134 ± 4 kDa was obtained from Vetec -Brazil. *Candida albicans* ATCC 10231 strain was obtained from the Universidade Católica Collection and was grown on liquid medium RPMI (Sigma-Aldrich, USA). Mouse macrophage RAW 264.7 cells were purchased from the ATCC (TIB-71) and cultured in DMEM medium supplemented with 10% FBS and 1% penicillin/streptomycin at 37 °C in 5% CO_2. Lipopolysaccharide (LPS) was obtained from InvivoGen. HUVECs (primary human

umbilical vein endothelial cells, Lonza) were cultured in endothelial basal medium 2 (EGM-2 BulletKit, Lonza) supplemented with growth factors (hFGF-β, hydrocortisone, VEGF, R3-IGF-1, ascorbic acid, heparin, FBS, hEGF).

Peptide synthesis and purity degree evaluation

The peptide was purchased from enterprise Peptide 2.0 Incorporated [8] which synthesized the peptide with 95% of purity. Cm-p1 molecular mass was confirmed by using MALDI-ToF MS/MS analysis (Autoflex, Bruker Daltonics, Billerica, MA). Purified peptide was solubilized in a minimum water volume and blended with an α-cyano-4-hydroxycinnamic acid saturated matrix solution (1:3, v:v), spotted onto a MALDI ToF target plate and air-dried at room temperature for 10 min. The α-cyano-4-hydroxycinnamic acid matrix solution was made at 50 mM in H_2O:ACN:TFA (50:50:0.3, v:v:v). Peptide monoisotopic mass was gained in the reflector mode with external calibration, using the Peptide Calibration Standard II (up to 4,000 Da mass range, Bruker Daltonics, Billerica, MA). The synthetic peptide concentrations were obtained by using the measurement of absorbance at 205, 215 and 225 nm, as defined by Murphy and Kies (1960).

Electrospun nonwoven mats of PVA/peptide.

Different concentrations of Cm-p1 (2.5 %, 5 % and 10 %, w/v) were solubilized in 0.5 ml of deionized water and stirred overnight at 70 ° C. After 12 h, 50 mg of PVA were slowly added in order to produce a 10% w/v solution and stirred at 70 °C until complete solubility. The electrospinning process was carried out on a horizontal configuration; a 1 mL plastic syringe with a stainless steel capillary (BD, gauge 12) was loaded with the PVA/polypeptide solution and processed at 15 kV supplied by a high voltage source (homemade), with a flow of 0.2 ml.h^{-1} using a syringe pump (NE-2000, New Era, Pump Systems Inc.) and a working distance of 10 cm from the needle tip to collector. The produced mats were collected on aluminum foils.

Scanning electron microscopy

For morphological analysis of nanofibers by scanning electron microscopy (SEM), a Zeiss DSM 962 (Carl Zeiss, Germany) microscope was used. Nanofiber samples of the cover slip were affixed to the surface of stubs, using double-sided adhesive conductive carbon tape. Stubs were covered with an ultra-thin gold layer (20 nm) using the Sputter Coat Emitech K550. SEM images were analyzed and captured, and the diameter of the fibers in the mats was determined using 10,000x magnification by Image J Tool for Windows version 3.0. Statistical analysis was performed using Microsoft Excel, one-way analysis of variance (ANOVA).

Atomic force microscopy measurements

Atomic force microscopy (AFM) images were obtained on a JPK Instruments Nanowizard II (Berlin, Germany) mounted on a Carl Zeiss Axiovert 200 inverted microscope (Jena, Germany). Images were performed in intermittent contact mode (air) using ACL silicon cantilevers from AppNano (Huntingdon, UK) with a tip radius of 6 nm, resonant frequency of approximately 190 kHz and spring constant of 58 N/m. All images were obtained with similar AFM parameter (setpoint, scan rate and gain) values. The scan rate was set between 0.3 and 0.6 Hz and setpoint close to 0.3 V. Height and error signals were collected and images were analyzed with the JPK image processing software v. 4.2.53 (JPK Instruments).

Cm-p1-PVA nanofiber release analyses

The Cm-p1-PVA release characteristics were made using the *in vitro* elution method [21]. Samples with an area of 2 cm × 2 cm, cut from the electrospun membranes, were put in glass test tubes (one sample per test tube, total number = 3) with 1 mL of phosphate-buffered solution (0.15 mol.L^{-1}, pH 7.4) in each. The glass test tubes were kept at 37 °C for 24 h, after which the eluent was removed and evaluated. Fresh phosphate-buffered solution (1 mL) was added for

Nanoscale Accepted Manuscript

the following 24 h period, and the procedure was sustained for 15 days. Drug concentrations in the eluents were analyzed using the standard curve carried out in RP-HPLC. At the same time, samples with the same area cut from the nanofibers were put in glass test tubes (one sample per test tube, total number = 3) with 1 mL of phosphate-buffered solution (0.15 mol.L^{-1}, pH 7.4) in each. The glass test tubes were kept at 37 °C for 0.5, 1, 1.5, 2, 4, 8, 12 and 24 h, after which the eluent was collected and determined by the standard HPLC assay curve. For peptide quantification a standard curve was carried out with several amounts (0.2, 0.4, 0.6, 0.8 and 1.0 mg) of peptide weighed in analytical balance (AND GH-202, USA). The standard deviation for the sample weighed was of 5% for each application into C18 analytical column in linear gradient of 5 to 95 % of acetronitrile in 0.01 % of TFA. The line equation observed, y = 1297x + 201 with R^2 value of 0.996, was used to quantify the samples in all steps of release measurement.

Antifungal bioassays

Bioassay against fungi was performed by measuring fungal growth inhibition using the radial diffusion assay (RDA) [25]. Sabouraud dextrose plates were made by dissolving 10 g.L^{-1} peptone, 20 g.L^{-1} dextrose, and 4 % agar in distilled water, after which the solution was autoclaved. The test solutions were prepared from samples with an area of 2 cm × 2 cm, cut from the electrospun membranes put in glass test tubes containing 1 mL of autoclaved distilled water and then kept for 24 h at 37 °C and 200 rpm. The samples were then lyophilized and solubilized with autoclaved distilled water. When the plates had hardened, circular holes were made in the medium with the large end of a 2-200 μL pipette tip. Into these holes, 20 μL of the solutions to be tested were added. 10 mL agarose Sabouraud dextrose solution was then mixed with a suspension of 5 mL of overnight grown fungi, after which it was poured into Petri dishes yielding a thickness of approximately 2 mm, and then the plates were set to incubate at 37 °C. Amphotericin B (30 μg.ml^{-1}) was used as the positive control. The following day, the plates were inspected for antimicrobial activity against the fungal strain. The activity was recognized as a clear zone of inhibition around the hole, and the larger the diameter of this ring, the higher the activity of the loading agent against this strain by Image J Tool

for Windows version 3.0. Statistical analysis was performed using Microsoft Excel, one-way analysis of variance (ANOVA).

Nanoscaffold/peptide immune toxicity analysis toward mammalian cells.

Plasma treated nanoscaffold surfaces with different nanofiber formulations (0.3 cm^2) were inserted into each well of a 96-well plate. Plasma surface chemical treatment using plasma reactor was done to improve the surface hydrophilicity and cell adhesion properties of the polymeric nanoscaffolds. The peptide/polymer ratio used in these experiments was (2.5%, 5% and 10%), the same ratio observed in the antimicrobial analysis. Plasma treatment was used to improve surface of nanoscaffold hydrophilicity. This procedure was followed by addition of RAW 264.7 macrophages with 2 x 10^3 cells.well^{-1} and grown for 24 h. As controls, positive control RAW cells were treated with 100 ng.mL^{-1} of LPS. ELISA assays (SA Biosciences) of the conditioned media from different groups were carried out according to the manufacturer's protocol to quantify the secreted cytokines IL-6 and TNF-α by the RAW cells. Each experiment was performed in triplicate [54-56].

Cell viability assays

In a similar way, cell viability of HUVECs in the presence of different nanoscaffolds was measured with Cell Titer 96 Aqueous Non-Radioactive Cell Proliferation MTS Assay (Promega) according to the manufacturer's protocol. To maintain the same standardization, the same peptide/polymer ratio (2.5%, 5% and 10%), was used in this assay. For this, the 2 x 10^4 HUVECs were grown on the different nanoscaffold groups and the absorbance was measured using plate reader at 490 nm after 24 h of cell culture. Each experiment was performed in triplicate [57].

Superoxide production analyses

Intracellular production of superoxide by HUVECs due to exposure to peptide/nanoscaffolds was evaluated using intracellular reactive oxygen species (ROS) assay (Cell Biolabs, Inc) according to the manufacturer's instructions. Similar to the above-mentioned experimental method, 2×10^4 HUVECs were grown on the nanoscaffolds for 24 h and fluorescence signals in each well were quantified with fluorometric plate reader at 480 nm/530 nm. The assay uses a cell-permeable fluorogenic probe, 2′,7′-dichlorodihydrofluorescein diacetate, to trace the ROS. The fluorescence intensity in each well is directly proportional to the ROS level within the cell cytosol[58]. In a separate experiment, the cells growing on the scaffolds for 48 h were stained with cell-permeant calcein AM dye (Life Technologies) to trace viability.

Hemolytic activity

The hemolytic activity was performed according Bignami[59] (1993) and Tramer[60] (2012) with modifications. Earlier, 1 mL of fresh blood from BALB/c mice was fractionated by centrifugation and the red blood cells were recovered in 1 % (v/v) PBS. The suspension was washed three times with PBS and aliquoted in microtubes and in PVA and 2.5 %, 5 % and 10 % Cm-p1-PVA; after 24 h of release, nanofibers were added and set aside for 1 h. Saline solution and 0.1 % Triton X-100 were used as negative and positive control, respectively. After 1 h, microtubes were centrifuged (1000 g; 2 min) and the supernatant was applied in 96 well plate. The absorbance was measured using reader at 406 nm (Bio-Tek PowerWave HT, EUA).

ACKNOWLEDGEMENTS

NOTES AND REFERENCES

1. Taweechaisupapong, S.; Choopan, T.; Singhara, S.; Chatrchaiwiwatana, S.; Wongkham, S. *Journal of ethnopharmacology* **2005,** 96, (1-2), 221-226.
2. Costa, A. C.; Pereira, C. A.; Junqueira, J. C.; Jorge, A. O. *Virulence* **2013,** 4, (5), 391-9.
3. Sudbery, P.; Gow, N.; Berman, J. *Trends in microbiology* **2004,** 12, (7), 317-24.
4. Gow, N. A.; Hube, B. *Current opinion in microbiology* **2012,** 15, (4), 406-12.
5. Benjamin, D. K., Jr.; Hudak, M. L.; Duara, S.; Randolph, D. A.; Bidegain, M.; Mundakel, G. T.; Natarajan, G.; Burchfield, D. J.; White, R. D.; Shattuck, K. E.; Neu, N.; Bendel, C. M.; Kim, M. R.; Finer, N. N.; Stewart, D. L.; Arrieta, A. C.; Wade, K. C.; Kaufman, D. A.; Manzoni, P.; Prather, K. O.; Testoni, D.; Berezny, K. Y.; Smith, P. B.; Fluconazole Prophylaxis Study, T. *JAMA : the journal of the American Medical Association* **2014,** 311, (17), 1742-9.
6. Formosa, C.; Schiavone, M.; Martin-Yken, H.; Francois, J. M.; Duval, R. E.; Dague, E. *Antimicrobial agents and chemotherapy* **2013,** 57, (8), 3498-506.
7. Otte, J.; Vordenbäumen, S. *Polymers* **2011**, (3), 2010-2017.
8. Cândido, E. S.; Cardoso, M. H. S.; Sousa, D. A.; Viana, J. F. C.; Oliveira-Júnior, N. G.; Miranda, V.; Franco, O. C. *Peptides* **2014**, (55), 65–78.
9. Mendez-Samperio, P. *Advanced biomedical research* **2013,** 2, 50.
10. Lopez-Abarrategui, C.; Alba, A.; Lima, L. A.; Maria-Neto, S.; Vasconcelos, I. M.; Oliveira, J. T.; Dias, S. C.; Otero-Gonzalez, A. J.; Franco, O. L. *Current microbiology* **2012,** 64, (5), 501-5.
11. C.Lopez-Abarrategui; Alba, A.; Silva, O. N.; Reyes-Acosta, O.; Vasconcelos, I. M.; Oliveira, J. T.; Migliolo, L.; Costa, M. P.; Costa, C. R.; Silva, M. R.; Garay, H. E.; Dias, S. C.; Franco, O. L.; Otero-Gonzalez, A. J. *Biochimie* **2012,** 94, (4), 968-74.
12. Zou, Z.; Liu, T.; Li, J.; Li, P.; Ding, Q.; Peng, G.; Zheng, Q.; Zeng, X.; Wu, Y.; Guo, X. *Journal of Biomedical Materials Research A* **2014,** 102A, (5), 1286–1293.
13. Mandal, S. M.; Roy, A.; Mahata, D.; Migliolo, L.; Nolasco, D. O.; Franco, O. L. *The Journal of Antibiotics* **2014**.
14. Chronopoulou, L.; Sennato, S.; Bordi, F.; Giannella, D.; Nitto, A. D.; Barbetta, A.; Dentini, M.; Togna, A. R.; Togna, G. I.; Moschini, S.; Palocci, C. *Soft matter* **2014,** 10, (12), 1944-52.
15. Zahedi, P.; Rezaeian, I.; Ranaei-Siadat, S.; Jafari, S.; Supaphol, P. *Polymers for Advanced Technologies* **2010**, (21), 77–95.
16. Bao, J.; Yang, B.; Sun, Y.; Zu, Y.; Deng, Y. *Journal of biomedical nanotechnology* **2013,** 9, (7), 1173-80.
17. Abdelgawad, A. M.; Hudson, S. M.; Rojas, O. J. *Carbohydrate polymers* **2014,** 100, 166-78.
18. Dongargaonkar, A. A.; Bowlin, G. L.; Yang, H. *Biomacromolecules* **2013,** 14, (11), 4038-45.
19. Lalani, R.; Liu, L. *Biomacromolecules* **2012,** 13, (6), 1853-63.
20. Chenwen, L.; Ruoqiu, F.; Caiping, Y.; Zhuoheng, L.; Haiyan, G.; Daqiang, H.; Dehua, Z.; Laichun, L. *International Journal of Nanomedicine* **2013**, (8), 4131–4145.
21. Chen, D. W.; Hsu, Y. H.; Liao, J. Y.; Liu, S. J.; Chen, J. K.; Ueng, S. W. *International journal of pharmaceutics* **2012,** 430, (1-2), 335-41.

Nanoscale Accepted Manuscript

22. Chen, D. W.; Liao, J. Y.; Liu, S. J.; Chan, E. C. *International Journal of Nanomedicine* **2012,** 7, 763-71.

23. Dave, R.; Jayaraj, P.; Ajikumar, P. K.; Joshi, H.; Mathews, T.; Venugopalan, V. P. *Journal of Biomaterials Science* **2013,** 24, (11), 1305-19.

24. Ruckh, T. T.; Oldinski, R. A.; Carroll, D. A.; Mikhova, K.; Bryers, J. D.; Popat, K. C. *Journal of Materials Science: Materials in Medicine* **2012,** 23, (6), 1411-20.

25. Eriksen, T. H.; Skovsen, E.; Fojan, P. *Journal of biomedical nanotechnology* **2013,** 9, (3), 492-8.

26. Heunis, T.; Bshena, O.; Klumperman, B.; Dicks, L. *International journal of molecular sciences* **2011,** 12, (4), 2158-73.

27. Heunis, T. D.; Smith, C.; Dicks, L. M. *Antimicrobial agents and chemotherapy* **2013,** 57, (8), 3928-35.

28. Lindner, H. B.; Zhang, A.; Eldridge, J.; Demcheva, M.; Tsichlis, P.; Seth, A.; Vournakis, J.; Muise-Helmericks, R. C. *PloS one* **2011,** 6, (4), e18996.

29. Sarig, H.; Rotem, S.; Ziserman, L.; Danino, D.; Mor, A. *Antimicrobial agents and chemotherapy* **2008,** 52, (12), 4308-14.

30. Torres, N. I.; Noll, K. S.; Xu, S.; Li, J.; Huang, Q.; Sinko, P. J.; Wachsman, M. B.; Chikindas, M. L. *Probiotics and antimicrobial proteins* **2013,** 5, (1), 26-35.

31. Sridhar, R.; Sundarrajan, S.; Venugopal, J. R.; Ravichandran, R.; Ramakrishna, S. *Journal of Biomaterials Science* **2013,** 24, (4), 365-85.

32. Jia, Y.; Gong, J.; Gu, X.; Kim, H.; Dongd, J.; Shen, X. *Carbohydrate polymers* **2007,** 67, (3), 403–409.

33. Peresin, M. S.; Habibi, Y.; Vesterinen, A. H.; Rojas, O. J.; Pawlak, J. J.; Seppälä, J. V. *Biomacromolecules* **2010,** 11, (9), 2471-2477.

34. Liu, Y.; Bolger, B.; Cahill, P. A.; McGuinness, G. B. *Materials Letters* **2009,** 63, 419–421.

35. Yang, E.; Qin, X.; Wang, S. *Materials Letters* **2008,** 62, 3555–3557.

36. Agarwal, S.; Wendorff, J. H.; Greiner, A. *Polymer* **2008,** 49, 5603–5621.

37. Meinel, A. J.; Germershaus, O.; Luhmann, T.; Merkle, H. P.; Meinel, L. *European Journal of Pharmaceutics and Biopharmaceutics* **2012,** 81, (1), 1-13.

38. Zhang, L. L.; Huang, L. H.; Zhang, Z. X.; Hao, D. J.; He, B. R. *Chinese Medical Journal (English Edition)* **2013,** 126, (20), 3891-6.

39. Zeng, J.; Hou, H.; Wendorff, J. H.; Greiner, A. *Macromolecular Rapid Communications* **2005,** 26, 1557–1562.

40. Gohil, J. M.; Bhattacharya, A.; Ray, P. *Journal of Polymer Research* **2006,** 13, 161–169.

41. Hassounah, I. A.; Shehata, N. A.; Kimsawatde, G. C.; Hudson, A. G.; Sriranganathan, N.; Joseph, E. G.; Mahajan, R. L. *Journal of Biomedical Material Research A* **2013**.

42. Lee, J.; Lee, D. G. *Journal of Microbiology and Biotechnology* **2010,** 20, (8), 1192–1195.

43. Cao, W.; Zhou, Y.; Ma, Y.; Luo, Q.; Wei, D. *Protein Expression and Purification* **2005,** 40, 404-410.

44. Aerts, A. M.; Bammens, L.; Govaert, G.; Carmona-Gutierrez, D.; Madeo, F.; Cammue, B. P.; Thevissen, K. *Frontiers in microbiology* **2011,** 2, 47.

45. Guilhelmelli, F.; Vilela, N.; Albuquerque, P.; Derengowski, L. D.; Silva-Pereira, I.; Kyaw, C. M. *Frontiers in microbiology* **2013,** 4, 353.

46. Mello, E. O.; Ribeiro, S. F. F.; Carvalho, A. O.; Santos, I. S.; Cunha, M. d.; Santa-Catarina, C.; Gomes, V. M. *Current microbiology* **2011,** 62, 1209–1217.

47. Machado, J. R.; Soave, D. F.; Silva, M. V. d.; Menezes, L. B. d.; Etchebehere, R. M.; Monteiro, M. L.; Reis, M. A. D.; Corrêa, R. R.; Celes, M. R. *Mediators of inflammation* **2014,** 2014, 1-10.

48. Afshar, M.; Gallo, R. L. *Veterinary dermatology* **2013,** 24, (1), 32-38

49. Duplantier, A. J.; Hoek, M. L. v. *Frontiers in Immunology* **2013,** 4, 143.

50. Pinto, D.; Marzani, B.; Minervini, F.; Calasso, M.; Giuliani, G.; Gobbetti, M.; Angelis, M. D. *Peptides* **2011,** 32, (9), 1815-24.

51. Kindrachuk, J.; Jenssen, H.; Elliott, M.; Nijnik, A.; Magrangeas-Janot, L.; Pasupuleti, M.; Thorson, L.; Ma, S.; Easton, D. M.; Bains, M.; Finlay, B.; Breukink, E. J.; Georg-Sahl, H.; Hancock, R. E. *Innate immunity* **2013,** 19, (3), 315-27.

52. Dempsey, P. W.; Vaidya, S. A.; Cheng, G. *Cellular and Molecular Life Sciences* **2003,** 60, 2604-2621.

53. Brandelli, A. *Mini-Reviews in Medicinal Chemistry* **2012,** 12, (8), 731-41.

54. Cheng, Q.; Lee, B. L.; Komvopoulos, K.; Yan, Z.; Li, S. *Tissue engineering. Part A* **2013,** 19, (9-10), 1188-98.

55. Hasan, A.; Memic, A.; Annabi, N.; Hossain, M.; Paul, A.; Dokmeci, M. R.; Dehghani, F.; Khademhosseini, A. *Acta biomaterialia* **2014,** 10, (1), 11-25.

56. Prakash, S.; Khan, A.; Paul, A. *Expert opinion on biological therapy* **2010,** 10, (12), 1649-61.

57. Paul, A.; Elias, C. B.; Shum-Tim, D.; Prakash, S. *Scientific reports* **2013,** 3, 2366.

58. Koontz, J.; Kontrogianni-Konstantopoulos, A. *Journal of Biological Chemistry* **2014,** 289, (6), 3468-77.

59. Bignami, G. S. *Toxicon* **1993,** 31, 817-820.

60. Tramer, F.; Ros, T. D.; Passamonti, S. *Methods in molecular biology* **2012,** 926, 203-217.